AL BSF FOR THIN SCREENPRINTED MULTICRYSTALLINE SI SOLAR CELLS

A. Schneider, C. Gerhards, F. Huster, W. Neu, M. Spiegel, P. Fath, E. Bucher[1]
R.J.S Young[2], A.G. Prince[2], J.A. Raby[2], A.F. Carroll[3]
Author for correspondence: A. Schneider
[1]University of Konstanz, Faculty of Physics, P.O.Box X916, D-78457 Konstanz, Germany
Tel.: +49-7531-88-2082, Fax: +49-7531-88-3895 email: a.schneider@uni-konstanz.de
[2]DuPont iTechnologies, Coldharbour Lane, Frenchay, Bristol, United Kingdom BS16 1QD
Tel : +44-1-179-313-227, email Richard.Young@gbr.DuPont.com
[3]DuPont iTechnologies, 14 Alexander Dr., Research Triangle Park, NC, 27709 USA
Tel: +1-919-248-5322, email: Alan.F.Carroll@usa.DuPont.com

ABSTRACT: A screen printed BSF is commonly used for manufacturing high efficiency multicrystalline solar cells, with average efficiencies up to 15 % in production using PECVD SiN firing through process. One key for reducing costs and energy consumption of the production process is the use of thinner wafers reducing from the current average multicrystalline wafer thickness of 330-350 µm to significantly thinner wafers of the order of 200 µm thickness. One of the major material challenges using thinner wafers is the bow of the wafers after firing, which lead to problems during module production. Alternative rear side passivation methods such as boron BSF, silicon oxide or silicon nitride have not achieved the same performance as the Al BSF, furthermore Al provides additional benefits such as a means to assist hydrogen diffusion in to the bulk with PECVD SiN and gettering of impurities during firing. In this work we studied the electrical and mechanical performance of new aluminium pastes developed by Du Pont processed to give various Al print thicknesses and fired on wafers using a PECVD SiN_x:H anti-reflection coating. Aluminium pastes of different compositions were investigated to evaluate the influence on the bowing characteristics and the electrical performance of 200 µm thick wafers, sized 12.5 x 12.5 cm.
Keywords: BSF - 1: bowing - 2: screen printing - 3

1. INTRODUCTION

Silicon has the most significant share in the production costs of silicon solar cells, clearly then, a reduction in the thickness of the wafer without loss in electrical performance or functional performance is extremely desirable. There is a significant difference between the thermal expansion coefficients of aluminium and silicon that will lead to wafer bowing where the bending stress has been overcome. If the bow exceeds a value of 1.4 mm, problems with handling and wafer mounting will occur during module production. The module producer can resolve the problem of the bowed wafer by flattening the wafer during or before tabbing, however, the resultant process would be more expensive and the yield losses due to breakage may be very high further increasing unit costs.

Bowing is negligible (<0.5 mm) for 12.5x12.5 cm standard wafers of 330-350 µm thickness but increases for thinner wafers. Values up to 5.5 mm could be measured for standard industrially processed cells of 200 µm thickness, sized 12.5x12.5 cm. In Figure 1 we can see that for 98 cm^2 wafers the bow increases with decreasing wafer thickness for a constant Al thickness, using the equation discussed later, good agreement with theory can be achieved.

There are cell designs that are able to reduce the bow in a way that it would not affect module production. One way to do this is to print Al only locally on the back side and passivate the intermediate surface using a dielectric layer [1]. This approach, however, has not led to comparable results in an industrially compatible process.

In the present work, we investigated the influence of bowing of thin solar cells and their electrical performance using Al screen-printing pastes of different compositions and under different printing conditions.

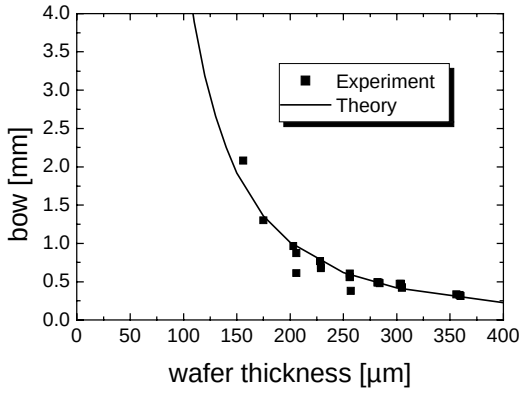

Figure 1 : Bowing as a function of cell thickness for standard solar cells with Al BSF, sized 98 cm² compared to the theoretical prediction based on a bimetallic strip model.

2. SOLAR CELL PROCESS

For all solar cells presented in this paper the following industrial process was applied:

1. Alkaline defect etching,
2. $POCl_3$ diffusion (35 Ω/□, to reach a wide processing window for different Al thicknesses),
3. PECVD SiN deposition,
4. Isolation by dicing off the edges,
5. Screen printed contacts (Ag front, Al rear)

The pastes were supplied by Du Pont. The best cell results so far obtained for thin wafers of 200 µm, sized 154 cm^2,

was an efficiency of η=15 %, J_{sc}=31.4 mA/cm^2, V_{oc}=612 mV and a fill factor of FF=78.1 %.

3. EFFECT OF CELL THICKNESS ON ELECTRICAL PERFORMANCE

Koval et al [2] found that cells exhibited higher efficiency for thinner cells relative to thicker cells with BSFs formed using aluminium pastes. In contrast, systems employing non-BSFs indicated declining performance. The performance improvement was reasoned to be due to increased optical reflection from the Al, reduced surface recombination velocity and an apparent increase in minority carrier diffusion length in the base of the cell.

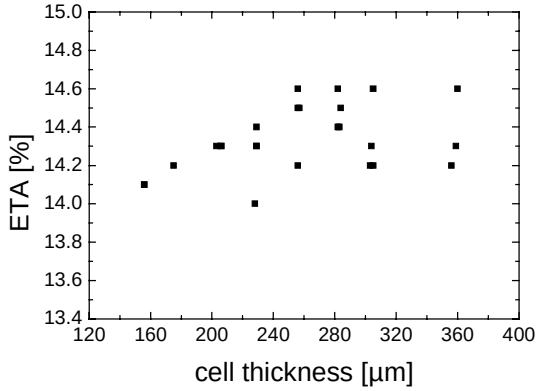

Figure 2: Change in efficiency as a function of cell thickness.

In the work reported here, Figure 2 shows how the efficiency changes as a function of cell thickness. It is not in agreement with the earlier observations of Koval et al; however, based on work reported later in this paper, it is likely that the Al deposit weight has a clear influence on the performance and will warrant further investigation with respect to electrical peformance as the wafer gets thinner.

4. EFFECTS OF AL DEPOSITION THICKNESS

4.1 Theoretical understanding of bowing due to Al deposition

Bowing will be observed when two or more layers of materials of different temperature expansion coefficients are in contact, in this case silicon and aluminium. The determining factors for bowing to become evident are the relative thickness of the layers, the dimensions of the two planes and the difference in temperature between the solidification point of one of the phases and the measured temperature. Simple models for the deflection are available [3] as shown in the following equation

$$\delta = \frac{3(\alpha_b - \alpha_a)(T_f - T)(t_b + t_a)d^2}{4t_b^{\,2}(4 + 6t_a/t_b + 4(t_a/t_b)^2 + (E_a/E_b)(t_a/t_b)^3 + (E_b/E_a)(t_b/t_a))}$$

where δ is the deflection (m), t_a is the thickness of the top layer (m), t_b is the thickness of the bottom layer (m), T_f is the firing temperature (°C), T is the measuring temperature (°C), α_a is the TCE for top component (10^{-6} K^{-1}), α_b is the TCE for the bottom component (10^{-6} K^{-1}), E_a is the elastic modulus for the top component (Pa), E_b is the elastic modulus for the bottom component (Pa) and d is the width of the smaller component (m). Using this equation, we obtain good agreement with experiment as shown in Figure 1.

4.2 Effect of Alumium print thickness

The printed Al thickness or laydown (in mg cm^{-2}) can be adjusted by changing the screen printing parameters or by changing the composition and rheology of the paste.

In the first part of this work (set 1), the deposit thickness (weight) was varied by the use of four screens with different theoretical paste volumes V_{Th} and in the second part of this work (set 2) we used the same screen but varied the paste composition and rheology to achieve a wider range of deposit thickness. In both sets, we used wafers of 200 µm thickness and 12.5x12.5 cm size.

The theoretical paste volume is equivalent to the volume of all mesh openings and indicates the theoretical wet layer thickness in µm. Two pastes, called A and B, with different compositions were investigated in this study. They were printed using different screens as summarized in Table I.

Table I: Effect of different screens on the paste laydown for two aluminium pastes under the same printing conditions (set 1).

screen	V_{Th}	m_{avg} paste A	m_{avg} paste B
	[cm^3/m^2]	[mg/cm^2]	[mg/cm^2]
1	43	9.92	11.9
2	36	8.05	9.44
3	30	8.44	9.61
4	24	7.27	8.46

4.2.1 Bowing results

Using different screens, Figure 3 shows the bow for cells fired under the same firing conditions (set 1) and measured as the height in mm from the horizontal should the wafer be perfectly flat as a function of the paste coverage for the two different pastes.

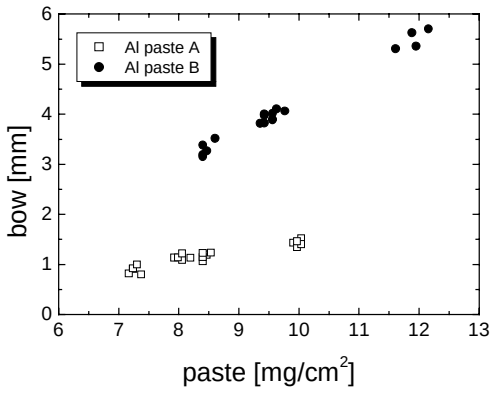

Figure 3: Bow vs. paste application for two different Al pastes (set 1). All cells were fired with the same firing conditions.

Figure 3 clearly shows that the paste composition has a greater effect on bowing than the deposit weight which also impacts bowing. In this case, paste B creates an unacceptable level of distortion for module construction even at relatively low paste weights whereas paste A gives significantly lower levels of distortion even at higher weight deposited.

The influence of Al fired thickness for pastes A and B for set 2, is shown in Figure 4 confirming that the paste composition has a greater effect on bowing compared to the fired thickness. We noted that for some of the thinner Al layers that there was a tendency towards ball formation which is known within the industry, it is also known that the ball formation is affected by the firing profile and the siliceous residues at the wafer surface and these become more dominating for the thinner layers. To measure the bowing and electrical parameters we removed these balls.

The interaction of the Al with the Si to make the BSF doping profile is formed by fast alloying and regrowth process according to the Al-Si phase diagram and not solid state diffusion [4]. The formation of the balls indicates that the Al has not alloyed with the silicon during the molten phase of the firing cycle and may result in a reduction of the BSF. During this study, we did not explore reduction of ball formation by using different firing profiles.

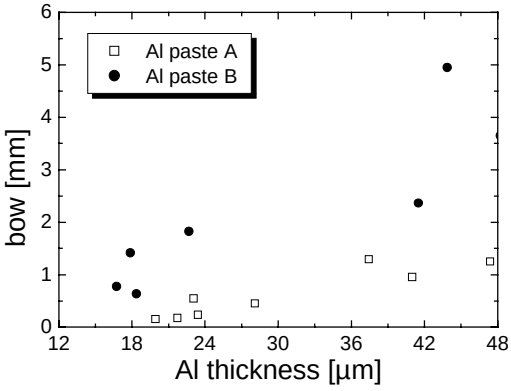

Figure 4: Bow as a function of fired Al thickness as observed for set 2.

4.2.2 Electrical performance

The influence of different printed Al thickness to cell performance has been discussed before [5] where the thickness of the p^+-layer, formed by the BSF, can be calculated as [6]

$$W_{BSF} = \frac{g_{Al}}{\rho_{Si}}\left(\frac{F}{100-F} - \frac{E}{100-E}\right)$$

where g_{Al} is the amount of Al deposited in g/cm^2, ρ_{Si} is the density of the silicon, F and E the percentage of Si mass in the liquid at the alloying and eutectic temperature.

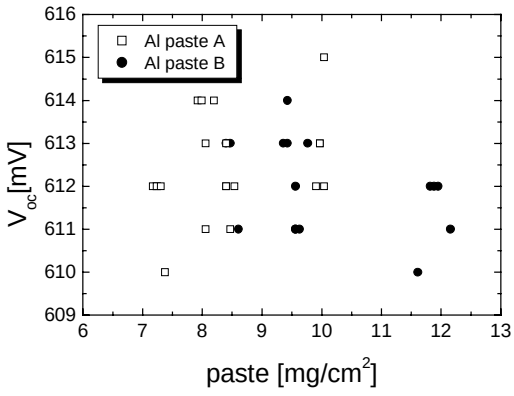

Figure 5: The effect of Al deposition thickness for set 1 of paste compositions A and B on V_{oc} fired under optimised conditions.

We would expect that by increasing the amount of printed Al we would see an effect on V_{oc} for cells with a diffusion length in the range of cell thickness. The influence of the print thickness for set 1 of pastes A and B on V_{oc} is shown in Figure 5. The firing parameters were optimised for each paste to allow the comparison of the cell parameters. The average cell efficiency was 14.5 % with a short circuit current of 31 mA/cm^2.

This work for set 1 showed no statistical correlation between the cell performance and the screen printed thickness between 7 and 13 mg cm^{-2} for pastes A and B. LBIC measurements and the comparison of other cell parameters confirm this statement. The absence of dependence of V_{oc} on print thickness could be because the BSF has reached an optimium thickness so that larger deposits do not result in further Si-Al interaction during the firing process. There is no point in making BSF much thicker than the diffusion length in the regrown layer [5]. To investigate the effect of thinner layers, we designed pastes that were used subsequently in set 2.

With the pastes designed for the experiments in set 2, we were able to access a wider range of Al deposit weights. Figure 6 shows that the open circuit voltage achieves a saturated value above a threshold aluminium weight but below this the V_{oc} reduces systematically. We see the same behaviour for pastes A and B with slightly better performance for paste A. We believe that this behaviour is caused by the difference in the Al available at the interface for alloying the composition of the Al-Si melt at peak temperature, the thicker layers provide sufficient Al to complete the Si-Al interaction. Higher or lower peak temperatures will influence the Al-Si composition and the dopant concentration of Al in Si [6]. For the cell manufacturer, the Al paste is the largest material cost element outside the Si wafer cost so better knowledge and control of the Al laydown has a profound influence on cost and performance.

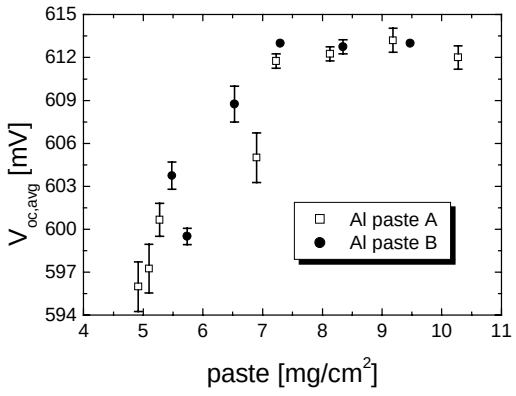

Figure 6: Dependence of V_{oc} to the paste consumption per wafer for set 2. All solar cells were fired with the same firing parameters to reach comparable values.

These findings do not agree with the prediction from the phase diagram [6] where the thickness of the back surface layer, W_{BSF} was expected to be proportional to the weight of Al deposited under constant firing conditions.

The highest cell efficiency achieved for set 2 was 15 % and was mostly limited by the material quality and the 35 Ω/□ emitter. Figure 7 presents the efficiencies obtained as a function of paste deposited for the different compositions A and B and show the same trends as for the V_{oc} discussed above.

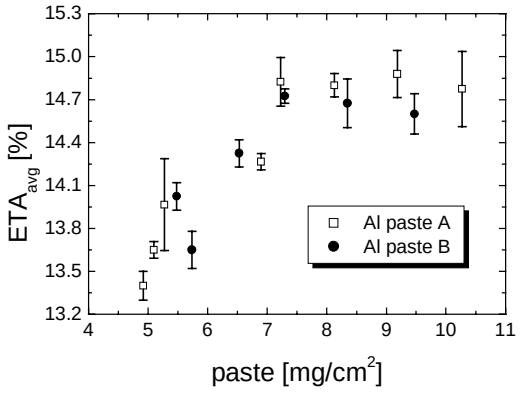

Figure 7: Dependence of efficiency to the paste consumption per wafer. A maximum efficiency of 15% was obtained.

4.2.3 LBIC results

Table II shows the LBIC results for cells with different Al weight deposits. The short circuit current J_{sc} at 980 nm increases continuously with Al deposit. This is in very good agreement with cell performance and furthermore confirms that the increase is due to better BSF quality. L_{eff} and IQE were extracted from LBIC data, using software [7]. An increase in L_{effavg} and IQE_{avg} is confirmed with heavier aluminium deposits.

Table II: LBIC data for cells with different Al weight deposits.

Al weight deposits	$J_{sc,avg}$ at 980 nm	L_{effavg}	IQE_{avg} at 980 nm
[mg/cm^2]	[mA/cm^2]	[µm]	
4.9	0.568	143	0.531
5.3	0.613	200	0.595
6.9	0.641	231	0.591
7.2	0.676	263	0.598
10.3	0.686	307	0.634

5. CONCLUSIONS

In this work we investigated the effect of aluminium paste composition and deposit thickness on the electrical performance and bowing tendency for thin wafers.

We demonstrated that the bow could be reduced by using lower print weights without adversely affecting the cell performance, an important finding for the cell manufacturer. More significantly, this work indicates that paste compositions exist that provide low bow performance enabling manufacturers to use 200 µm thick wafers.

In this work, we were not able to confirm that the back surface field formation is a proportional function of the weight of Al deposit.

6. ACKNOWLEDGEMENTS

The authors like to thank M. Keil for technical assistance in solar cell processing. The help of T. Pernau and B. Fischer during solar cell characterisation is also gratefully acknowledged.

REFERENCES

[1] B. Finkenstein, Proceedings of the 16th EC PVSEC, Glasgow, GB, 2000, p. 1394 – 1396
[2] T. Koval et al, Proceedings of the 25th PVSC, Washington, 1996, p. 505-507
[3] Roark and Young, Formula for Stress and Strain, 5th edition, McGraw Hill (19750, p. 113
[4] P. Loelgen et al, Proceedings of the 23rd IEEE PVSC, Louisville, 1993, p. 236
[5] P. Loelgen, doctor thesis, Universiteit Utrecht, 1995, p. 58
[6] J. del Alamo, J. Eguren and A. Luque, Solid State Electronics 24, (1981), p. 415
[7] T. Pernau et al., Proceedings of the 17th EC PVSEC, Munich, D, 2001